

Analytical Methods

Accepted Manuscript



This is an *Accepted Manuscript*, which has been through the Royal Society of Chemistry peer review process and has been accepted for publication.

Accepted Manuscripts are published online shortly after acceptance, before technical editing, formatting and proof reading. Using this free service, authors can make their results available to the community, in citable form, before we publish the edited article. We will replace this *Accepted Manuscript* with the edited and formatted *Advance Article* as soon as it is available.

You can find more information about *Accepted Manuscripts* in the [Information for Authors](#).

Please note that technical editing may introduce minor changes to the text and/or graphics, which may alter content. The journal's standard [Terms & Conditions](#) and the [Ethical guidelines](#) still apply. In no event shall the Royal Society of Chemistry be held responsible for any errors or omissions in this *Accepted Manuscript* or any consequences arising from the use of any information it contains.

Click synthesis of boronic acid-functionalized molecularly imprinted silica nanoparticles with polydopamine coating for enrichment of trace glycoprotein†

Cite this: DOI: 10.1039/x0xx00000x

Received 00th January 2012,
Accepted 00th January 2012

DOI: 10.1039/x0xx00000x

www.rsc.org/

Lixiang Sun,^a Danhong Lin,^b Guowei Lin,^b Ling Wang,^a Zian Lin^{a*}

A facile strategy based on synergistic effect of molecular imprinting and boronate affinity was proposed for glycoprotein imprinting. Polydopamine (PDA)-coated boronic acid-functionalized molecularly imprinted silica nanoparticles (MIPs) were prepared by “thiolene” click reaction using SiO₂ as core, 3-acrylamidophenyl boronic acid (AAPBA) as functional monomer, horseradish peroxidase (HRP) as glycoprotein template. Well defined core-shell structure of MIPs was obtained after self-polymerization of dopamine (DA) on the surface of HRP-immobilized silica nanoparticles (NPs). The polymerization conditions and adsorption behavior were investigated in detail in order to obtain the highest selectivity and binding capacity. Under the optimized conditions, the HRP-MIPs showed higher binding affinity towards HRP than non-imprinted nanoparticles (NIPs), and the corresponding adsorption capacity (Q) and imprinted factor (α) reached 0.58 $\mu\text{mol g}^{-1}$ and 2.6, respectively. The specificity for HRP recognition was evaluated with competitive experiment, and the result indicated the HRP-MIPs had higher selectivity for the template. The good features of the HRP-MIPs facilitated selective isolation and enrichment of trace HRP from human serum. In addition, the stability and regeneration were also investigated, which indicated the HRP-MIPs had excellent reusability.

Introduction

Glycoproteins are a large family of proteins that play important roles in numerous biological processes.¹ Analysis of glycoproteins may facilitate discovery of potential biomarkers.² Although mass spectrometry has proven to be a powerful tool for glycoprotein analysis, it is almost impossible to directly identify glycoproteins without any sample pretreatment. Many efforts have been devoted to address this issue in the past decade including lectin affinity chromatography, hydrophilic interaction chromatography, hydrazide chemistry, and boronate affinity chromatography.³⁻⁶ Although some achievements have been made, additional affinity approaches for highly efficient enrichment of glycoproteins are highly desirable.

Molecularly imprinted polymers (MIPs) are tailor-made synthetic receptors with high affinity and specificity towards the target analytes,^{7,8} which has found important applications in separation,^{9,10} sensing,^{11,12} and drug discovery.¹³ Imprinting of macromolecules, particularly proteins, is challenging due to conformational change of the templates during polymerization as well as difficulty of template removal.⁷ To overcome these difficulties, several strategies have been proposed for

imprinting proteins, such as metal coordination,^{14,15} epitope imprinting,^{16,17} and surface imprinting.¹⁸⁻²⁰ Among them, surface imprinting attracts great attention and displays the advantageous efficacy in protein imprinting because the imprinted sites can be close to or at the surface of MIPs and enable the elution and rebinding of the target protein easily, and therefore is regarded as the most promising strategy for protein imprinting. Many successful examples of surface imprinting (e.g. nanoparticles, nanowires/nanotubes, and quantum dots) have been published in recent years.²¹⁻²³ However, these approaches are not generally applicable since they were not designed on the basis of common features of all proteins or subclass of proteins.

Boronate affinity is a unique means for selective capture and enrichment of cis-diol containing biomolecules. The principle is that boronic acids form stable cyclic esters with cis-diol molecules under an alkaline aqueous solution and the cyclic esters dissociate when the environmental medium is changed to acidic pH. The unique switching property makes boronic acid promising affinity ligands in the recognition of glycoproteins. Many successful applications of boronic acid-based materials in glycoprotein recognition have been

presented in recent years.²⁴⁻²⁶ Nevertheless, making a clear and unambiguous differentiation between glycoproteins remains a great challenge due to the unbiased affinity of boronic acids towards all kinds of glycoproteins. More recently, an encouraging breakthrough in selective recognition of glycoproteins via boronate affinity molecular imprinting strategy was achieved by Liu's group,²⁷ in which the boronate affinity MIPs, synthesized by free radical polymerization, exhibited excellent recognition towards target glycoproteins. Subsequently, the same groups developed a series of boronate affinity MIPs for glycoprotein recognition and detection.²⁸⁻³² Besides, our group³³ and Zhang et al.³⁴ also developed the boronate affinity MIPs for glycoprotein recognition based on the same synthetic procedure. Although some advantages were shown, self-polymerization of vinyl-containing functional monomers with affinity ligands is unavoidable, which would potentially have negative effect on glycoprotein recognition.

Thiol-ene reaction, as an important segment of "click chemistry", has been established as one of the most reliable approaches for covalent assembly of various molecules. Because of its good chemoselectivity and high conversion, the thiol-ene reaction has been widely applied in surface science and bioconjugation.³⁵ In principle, introducing the affinity ligands of boronic acid onto the surface of matrices via thiol-ene click reaction can avoid the self-polymerization of vinyl-containing boronic acids,^{36,37} and potentially improve the orientated assembly of template and recognition performance of MIPs. Despite its attractive features, employing click reaction strategy for synthesis of boronate affinity MIPs have not been reported so far. On the other hand, the observation of the adhesion of invertebrate mussels to solid surfaces led to the rapid development of polydopamine (PDA) in surface chemistry.³⁸ As a novel coating material, PDA processes excellent biocompatibility and can be easily deposited on virtually all types of inorganic and organic substrates. Over the past few years, several applications of introducing PDA coating into protein imprinting have been demonstrated successfully.^{19,39,40}

Herein, a facile strategy based on the combination of molecular imprinting and boronate affinity was proposed for glycoprotein imprinting. The core-shell structure of boronic acid-functionalized imprinted silica nanoparticles (MIPs) obtained by "thiol-ene" click reaction and coated with thin adherent PDA layer can facilitate the orientated assembly and easy removal of the template glycoprotein. The recognition performance of the MIPs was evaluated by investigating the binding kinetics, binding capacity, specificity and recovery for the template glycoprotein. In addition, the practicability for biological application was further assessed by selective isolation and enrichment of trace horseradish peroxidase (HRP) from human serum.

Materials and methods

Materials

γ -Mercaptopropyltrimethoxysilane (γ -MPTS) and tetraethoxysilane (TEOS) were purchased from Chemical Factory of Wuhan University (Wuhan, China). 3-Acrylamidophenylboronic acid (AAPBA) and dopamine (DA) was obtained from Beijing J&K Chemical Technology Co. Ltd. HRP (Mw 44 kDa, pI 7.5), bovine serum albumin (BSA; Mw 66.4 kDa, pI 4.9), concanavalin A (Con A; 102 kDa, pI 4.5-5.5), human transferrin (Trf; 80 kDa, pI 5.5) and trypsin (Try; 23.3 kDa, pI 10.8) were purchased from Shanghai Lanji Co. Ltd. (Shanghai, China). 3,3',5,5'-Tetramethylbenzidine (TMB) was purchased from Sinopharm Chemical Reagent Co., Ltd. (Shanghai, China). Other reagents were of analytical grade or better. Deionized water was prepared with a Milli-Q water purification system (Millipore, Milford, MA). All proteins were dissolved in phosphate buffer (PBS, 10 mM, pH 9.0) at a concentration of 1.0 mM as stock solutions, and diluted to the desired concentration with PBS. Healthy human serum sample was kindly donated from Fujian Province Official Hospital (Fuzhou China). The study protocol and written informed consent were approved by the Fujian Province Official Hospital Ethics Committee (2014-KFFJJ-PT-2). All serum-related experiments were performed according to the Declaration of Helsinki.

Synthesis of SiO₂@SH@AAPBA

The synthetic procedure of monodisperse SiO₂ NPs was as follow. In brief, 6 mL of TEOS was added to the mixture of 100 mL of ethanol, 4 mL of deionized water and 3.2 mL of ammonia aqueous solution (25%) with vigorous stirring at 30 °C and the reaction was continued for 24 h. Subsequently, the resultant colloidal SiO₂ NPs were modified with γ -MPTS to obtain clickable thiol groups on the surface. Briefly, 2.0 mL of γ -MPTS was added dropwise and then the coating of SiO₂ NPs with thiol groups was obtained by stirring the mixture for 24 h (denoted as SiO₂@SH NPs) Finally, the as-prepared SiO₂@SH was washed three times with water, and then dried.

600 mg SiO₂@SH NPs were dispersed in 40 mL methanol in a round bottomed flask. Then 120 mg AAPBA and AIBN (1%, w/w) were added and the reaction mixture was stirred for 12 h at 72 °C under N₂ atmosphere. The resultant AAPBA-immobilized SiO₂ NPs (denoted as SiO₂@AAPBA NPs) were washed several times with deionized water, and then dried.

Synthesis of HRP-imprinted silica nanoparticles

For the preparation of HRP-imprinted SiO₂ NPs (HRP-MIPs), HRP (8 mg) was dissolved in 15 mL PBS (10 mM, pH 9.0) containing SiO₂@AAPBA (200 mg), and then the solution was shaken for preassembly at room temperature for 3 h. After adding 25 mg DA, the solution was incubated for 24 h at room temperature. After the reaction, the HRP-MIPs were collected by centrifugation and then washed with deionized water to remove unreacted monomers. Afterwards, the HRP-MIPs were washed repeatedly with the solution containing Tween 20 (0.1%, v/v), mercaptoethanol (5%, v/v) and acetic acid (10%, v/v) to remove the embedded template until no HRP in the supernatant was detected using UV/Vis spectrophotometer at

403 nm. Subsequently, the HRP-MIPs were rewashed several times with deionized water to remove residual Tween 20, mercaptoethanol and acetic acid. Finally, the HRP-MIPs were dried at room temperature for further use. Similarly, the nonimprinted SiO_2 NPs (NIPs) was prepared following the same procedure in the absence of the template HRP.

SDS-PAGE analysis of proteins.

5 mg of the HRP-MIPs and NIPs were individually immersed with 500 μL of protein mixture (containing 10.0 μM HRP and 15.0 μM BSA), After gentle shaking for 1 h at room temperature, the resultant HRP-MIPs and NIPs were firstly washed with 2 mL of 30% (v/v) ACN/ H_2O solution to remove nonspecifically adsorbed proteins. Then the HRP-MIPs and NIPs that bound HRP were eluted with the solution containing Tween 20 (0.1%, v/v), mercaptoethanol (5%, v/v) and acetic acid (10 %, v/v) for 30 min, and then the supernatant was collected and analyzed by SDS-PAGE.

Real sample preparation and colorimetric detection.

3 mg of the HRP-MIPs and NIPs were individually immersed with 500 μL diluted human serum (100-fold dilution with 0.01 M PBS at pH9.0) spiked with 10 ng mL^{-1} HRP. After incubation at room temperature for 1 h, the HRP-MIPs and NIPs were washed three times with 30% (v/v) ACN/ H_2O to remove non-binding proteins. Afterwards, the HRP-MIPs and NIPs were eluted by using 50 μL acetic acid (5%, v/v) containing Tween 20 (0.1%, v/v) as the eluting solvent. Finally, the eluate was collected for UV/vis spectral analysis.

100 μL of TMB solution and 100 μL of H_2O_2 were mixed with 10 μL of real samples (or the supernatant and the eluate) in each centrifugal tube, which were incubated for 6 min at room temperature. Then, the reaction is terminated by addition of 50 μL of 2 M H_2SO_4 . Finally, the absorbance was detected using UV/Vis spectrophotometer at the wavelength of 450 nm.

Regeneration of the imprinted silica nanoparticles

5.0 mg each of the HRP-MIPs and NIPs were added to 2.5 mL of 10.0 μM HRP solution and stirred for 1 h at room temperature. After centrifugation, the recovered HRP-MIPs and NIPs were washed with the solution containing Tween 20 (0.1%, v/v), mercaptoethanol (5%, v/v) and acetic acid (10%, v/v) to ensure complete removal of the residual HRP. Then, the HRP-MIPs and NIPs were washed several times with deionized water. The recovered product was then reused for adsorption of HRP.

Results and discussion

Preparation and characterization of HRP-imprinted silica nanoparticles

The general scheme for the synthesis of glycoprotein-imprinted silica NPs was illustrated in Fig.1, it involves the first synthesis of uniform SiO_2 NPs by using TEOS as sole precursor and the subsequent attachment of clickable SiO_2 @SH NPs by sol-gel

reaction of γ -MPTS. The key to the success of this strategy is the introduction of AAPBA onto the surface of SiO_2 @SH NPs via thiol-ene click reaction, which allows the easy and orientated assembly of the template (HRP) by reversible covalent binding in basic medium. The click strategy also proved to have a great effect on the template immobilization and selectivity. Afterwards, a thin and adherent PDA layer covering HRP-conjugated SiO_2 @AAPBA NPs was formed by self-polymerization of DA under mild conditions. Finally, removal of the target molecules led to the imprinted 3D cavities. The self-polymerization process of DA was found to play an essential role in template recognition. Herein, the polymerization time and concentration of DA were investigated in detail. The result (data not shown) that the polymerization time less than 8 h exhibited little imprinting recognition, possible reason was that the thickness of PDA layer was very thin (< 2-3 nm), which reduced the recognition sites. Based on this consideration, 12h was adopted in order to ensure that the HRP-MIPs have enough recognition sites and the stability of PDA layer. Besides, the HRP-conjugated SiO_2 @AAPBA NPs were incubated for 12 h with DA at different concentration (6.67, 3.33, 1.67, and 1.0 mg mL^{-1}). It was observed (Fig.S1 in the ESI†) that the adsorption capacity (Q) of the HRP-MIPs towards HRP gradually increased with the decrease of DA concentration, suggesting that thin PDA coating facilitated high Q. However, the Q of the NIPs towards HRP kept constant with DA varying from 6.67 to 1.67 mg mL^{-1} and promptly increased with DA of 1.0 mg mL^{-1} and their corresponding imprinting factors (α) were 1.32, 1.64, 2.40 and 1.02, respectively. Based on the results, 1.67 mg mL^{-1} DA was chosen as the best for further studies.

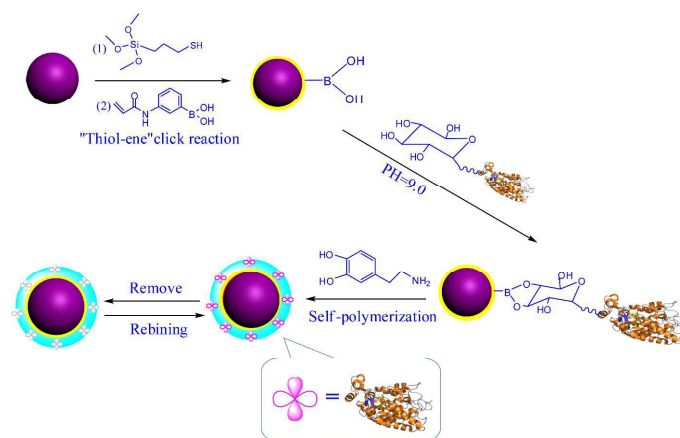


Fig. 1 Click synthesis of boronate affinity molecularly imprinted silica nanoparticles with PDA coating and its recognition mechanism toward glycoproteins.

Fig.2 shows the typical TEM images of the SiO_2 NPs, SiO_2 @AAPBA, and HRP-MIPs, respectively. It was observed from Fig.2(A-B) that the SiO_2 NPs had good dispersibility and the average diameter of 50 nm. Presented in Fig.2(C-D) was the images of SiO_2 @AAPBA NPs, which had a uniform size with an average diameter of 60 nm, about 20% larger than that of the bare SiO_2 NPs. Fig.2(E-F) revealed that the core-shell structure

of the HRP-MIPs was successfully prepared by self-polymerization of DA. Furthermore, the surface of the HRP-MIPs become rougher and its corresponding diameter increased to 70 nm, indicating that the PDA layer was an average of 5 nm in thickness. Fourier transform infrared (FT-IR) spectroscopy also provides a direct proof for the synthetic process (Fig.S2 in the ESI†). In addition, the surface area, pore volume and average pore diameter were measured by Brunauer–Emmett–Teller (BET) method and the total surface area of the HRP-MIPs was 45.79 m² g⁻¹, while that of the NIPs was only 37.96 m² g⁻¹. Pore volumes of the HRP-MIPs and NIPs were found to be 0.381 and 0.355 cm³ g⁻¹. Average pore diameter of the HRP-MIPs and NIPs were 33 and 37 nm, respectively. The difference in surface area and pore volume of the HRP-MIPs compared with the NIPs mainly thanks to the formation of imprinting sites after removal of template.

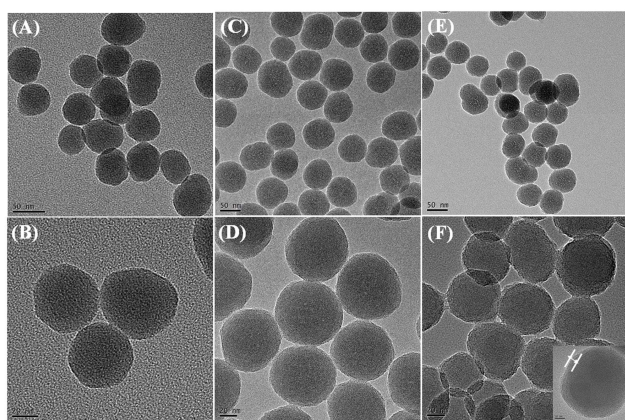


Fig. 2 TEM images of (A-B) SiO₂ NPs; (C-D) SiO₂@AAPBA NPs; (E-F) HRP-MIPs. Scale bar: 50 nm for A, C and E; 20 nm for B, D and F; 10 nm for inset.

Adsorption isotherms

The binding experiments were performed at different initial concentrations of HRP, ranging from 0 to 11.5 μM, to compare the Q of the HRP-MIPs against NIPs. At the early experiment, we are not sure what the exact incubation time is. So the incubation time was set at 12 h, which was sufficient to ensure the adsorption completely. As shown in Fig.3(A), the Q of HRP on HRP-MIPs gradually increased with the increase of HRP concentration from 0 to 10.0 μM, and came to saturation over 10.0 μM. In this case, the experimental Q_{max} was 0.58 μmol g⁻¹. In contrast, the NIPs showed low affinity towards HRP and its corresponding Q_{max} was 0.21 μmol g⁻¹. The result could be explained that the imprinting process in the HRP-MIPs could form specific recognition cavities that showed high affinity towards HRP. It should be noted that although DA is not the best choice as functional monomer for boronic acid-based molecule imprinting because of the competition effect generated by its strong boronate affinity with boronic acids²⁸, the excellent hydrophilicity and biocompatibility as well as fine controllable polymerization are very suited for hydrophilic glycoprotein. The result obtained from Fig.3(A) also supported the view that the imprinting occurred in HRP-MIPs. In

addition, linear regression analysis was performed to determine model parameters, and the results (Fig.S3 in the ESI†) demonstrated that Langmuir adsorption model was well fitted for HRP adsorption within the concentration ranges studied. The theoretical Q_{max} was calculated to be 0.91 μmol g⁻¹, approximately 3-fold higher than that obtained in the NIPs, where the theoretical Q_{max} of 0.32 μmol g⁻¹ was obtained. Accordingly, the α value was 2.84. Although the α value obtained in current work increased slightly, the NIPs prepared by thiol-ene click reaction showed lower nonspecific adsorption towards HRP than that of our previous work, where the theoretical Q_{max} of 0.52 μmol g⁻¹ was obtained with the NIPs synthesized by free radical polymerization,³³ demonstrating its superiority of this imprinting strategy.

Adsorption kinetics

The adsorption kinetics were also studied. The HRP-MIPs took up 90% of the equilibrium amount within 30 min, and the total equilibrium time was shorter than 60 min (Fig.3(B)). The rebinding rate of the HRP-MIPs is exceedingly rapid, compared to the previous works.^{41,42} The fast kinetics can be attributed to the thin PDA coating created over SiO₂@AAPBA NPs and strong boronate affinity interaction. As for the NIPs, however, lower Q and longer adsorption time (~100 min) were obtained, indicating that the NIPs had no imprinted cavities, and showed the main adsorption behaviour of nonspecific binding.

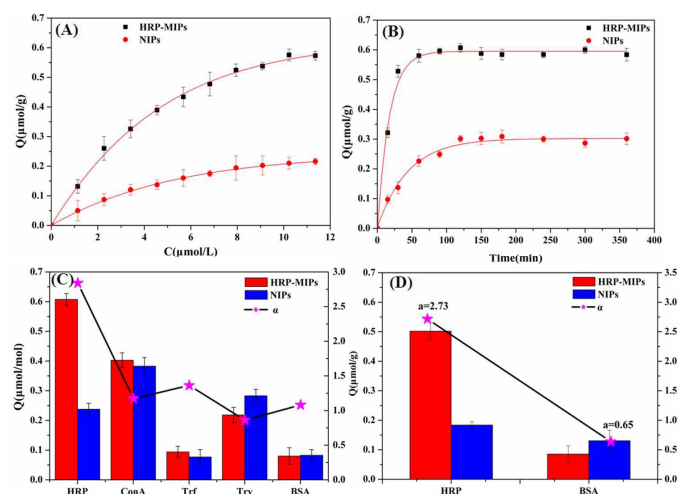


Fig. 3 (A) Adsorption isotherms, (B) adsorption kinetics, (C) single protein binding, and (D) competitive binding experiments.

Amount of HRP-MIPs and NIPs: 1 mg; volume: 1 mL; binding media: 0.01 M PBS (pH 9.0); C_{HRP}: 0–11.5 μM, incubation time: 12 h for (A) experiments; C_{HRP}: 10.0 μM for (B) experiments; the concentration of each protein, 10.0 μM and incubation time: 1 h for (C) and (D) experiments; The points represent mean values of three measurements.

Rebinding specificity

To evaluate the selectivity of the HRP-MIPs towards HRP, four proteins with different pI, Mw and glycosylated moiety, including the glycoproteins (Con A and Trf) and nonglycoproteins (Try and BSA), were selected as the competitive proteins. Presented in Fig.3(C) was the binding

capacities of the HRP-MIPs and NIPs for the tested proteins with a feed concentration of 10.0 μM . It was observed that the HRP-MIPs exhibited high affinity towards HRP with respect to the NIPs, and its corresponding α reached 2.76, much higher than those of the competitive proteins, where the α values for Con A, Trf, Try and BSA were 1.05, 1.22, 0.78 and 0.97, respectively. Significantly, the Q of the HRP-MIPs towards HRP was highest in all tested proteins. The specificity can be attributed to the synergistic effect of molecular imprinting and boronate affinity.

To further illustrate the specificity, a binary competitive adsorption experiment was performed with BSA as the competitor in the coexistence of equivalent template. As shown in Fig.3(D), the HRP-MIPs exhibited high affinity towards HRP even in the presence of BSA, indicating that the coexisted protein have no effect on the target recognition. In addition, the selective isolation of HRP from protein mixture was also examined by SDS-PAGE analysis. Fig.4 displayed the electropherogram of protein mixture before and after treatment with the HRP-MIPs and NIPs, respectively. Two major bands in the lane 2 presented the mixture of HRP and BSA. After treatment with the HRP-MIPs, the supernatant was detected and the result (lane 3) showed that the band of HRP faded evidently and the remainder changed little, confirming that the majority of HRP was selectively captured by the HRP-MIPs. Meanwhile, only a dark band of HRP (lane 5) appeared after elution. In contrast, no obvious color change was observed in lane 4 after treatment with the NIPs, and no band were detected in lane 5 after elution. The above results indicated again that the HRP-MIPs had specific affinity towards HRP, which give us more confidence for exploring its application potential in complex biological sample.

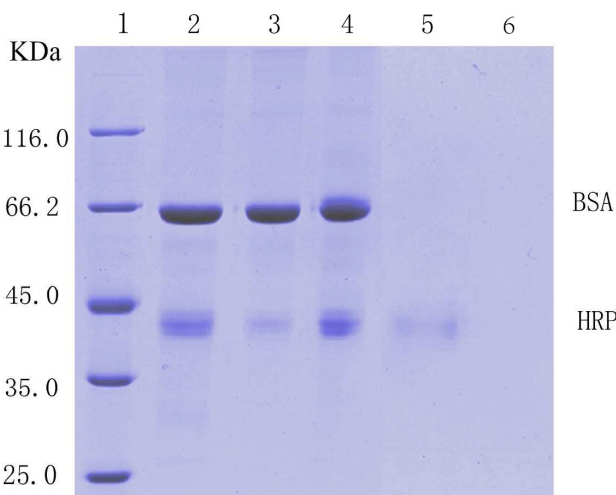


Fig. 4 SDS-PAGE analysis of model proteins before and after treatment with HRP-MIPs and NIPs.

Lane (1) Mark model proteins; (2) mixtures (10.0 μM HRP, and 15.0 μM BSA); (3) the supernatant after treatment with HRP-MIPs; (4) the supernatant after treatment with NIPs; (5) the eluate from HRP-MIPs; (6) the eluate from NIPs, loading amount of protein mixtures: 10 μL .

Application

The feasibility of the prepared HRP-MIPs was demonstrated by selective enrichment of trace HRP from diluted human serum spiked with 10 ng mL^{-1} HRP. Combined with colorimetric detection, a simple and sensitive MIP-based visualization method permitted the specific quantification of trace HRP in human serum. Fig.5(A) (and Table.S1 in the ESI†) demonstrated that about 74.2% HRP was extracted from human serum by using HRP-MIPs as sorbent, 2.7 times higher than that obtained with NIPs ($\sim 27.2\%$). The result was well in agreement with the theoretical α value as mentioned above. Moreover, a clear color changes were observed from Fig.5(A) by comparing human serum before and after treatment with the HRP-MIPs and NIPs. Compared with that from the NIPs, an unambiguous blue color was observed in eluate from HRP-MIPs. UV/vis spectra also supported the color changes (Fig.5(B)). It should be noted that only 30% HRP was eluted from HRP-MIPs, even though 2 times higher than that obtained from NIPs. The low recovery is mainly due to the use of acetic acid/Tween 20 as eluting solvents in order to reach a compromise with TMB- H_2O_2 detection system.

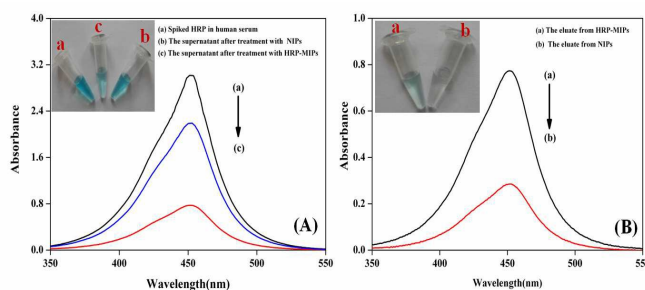


Fig. 5 (A) UV/vis spectroscopy assay of human serums spiked with 10 ng mL^{-1} HRP and (B) their corresponding eluate.

The experimental conditions are same as Fig.3.

Regeneration and reproducibility

The stability and regeneration of the HRP-MIPs were examined by six consecutive cycles of adsorption-desorption experiments. The results (Fig.S4 in the ESI†) demonstrated that the HRP-MIPs and NIPs remained stable for up to six adsorption cycles with little changes of Q and α , demonstrating the excellent stability.

Method validation

The recognition mechanism was further explored by comparing different imprinting strategies. One strategy is the proposed method (route A) described in current work. Another one is based on the same protocol without click addition of AAPBA (route B). Fig.6 showed that route B had no imprinting effect on HRP in comparison to route A, where the Q and α was lower than those obtained in route A, convincingly demonstrating that AAPBA is a critical parameter affecting the formation of recognition sites. One the other hand, the $\text{SiO}_2@\text{SH}@\text{AAPBA}$ NPs without coating PDA showed no selectivity towards the target template (data not shown). The above results confirmed

again that the synergistic effect of molecular imprinting and boronate affinity responded to the recognition of the target glycoprotein.

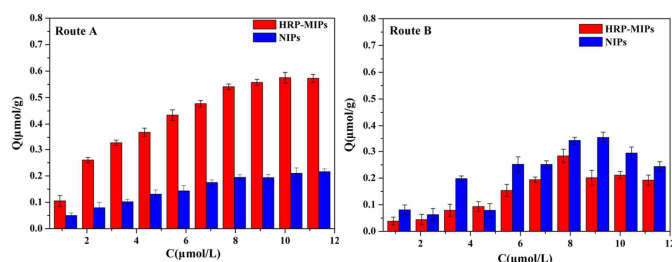


Fig.6 Effect of two different synthetic routes on the imprinting of the HRP-MIPs and NIPs.

Amount of HRP-MIPs and NIPs: 1 mg; volume: 0.5 mL; binding media: 0.01 M PBS (pH 9.0); incubation time: 2 h; C_{HRP} : 10.0 μM . The points represent mean values of three measurements.

Conclusions

In this work, a facile click reaction strategy was developed for synthesis of boronic acid-functionalized molecularly imprinted silica nanoparticles with polydopamine coating. The as-prepared imprinted silica nanoparticles displayed good dispersibility and well-defined core-shell structure. Due to the unique properties of molecular imprinting combining with boronate affinity, the HRP-MIPs exhibited large adsorption capacity, fast adsorption kinetics, and high selectivity towards the target glycoprotein in comparison with NIPs. In addition, the successful application in enrichment of trace HRP from human serum by using HRP-MIPs suggests its potential in glycoproteomic analysis.

Acknowledgements

This study was supported by the National Natural Science Foundation of China (21375018), and the Natural Science Foundation of Fujian Province (2014J01402).

Notes and references

a: Ministry of Education Key Laboratory of Analysis and Detection for Food Safety, Fujian Provincial Key Laboratory of Analysis and Detection Technology for Food Safety, College of Chemistry, Fuzhou University, Fuzhou, Fujian 350116, China.

b: Fujian Health College, Fuzhou, Fujian 350101, China.

E-mail: zianlin@fzu.edu.cn (Z.A. Lin); Fax: +86-591-22866135

† Electronic Supplementary Information (ESI) available. See DOI: 10.1039/b000000x/

- 1 L. Krishnamoorthy and L.K. Mahal, *ACS Chem Biol.* 2009, **4**, 715-732.
- 2 D. L. Meany, Z. Zhang, L.J. Sokoll, H. Zhang and D.W. Chan, *J. Proteome Res.* 2009, **8**, 613-619.
- 3 Y. Li, P. Shah, A.M. De Marzo, J.E. Van Eyk, Q.Q. Li, D.W. Chan and H. Zhang, *Anal. Chem.*, 2015, **87**, 4683-4687.
- 4 J. Zhu, F. J. Wang, R. Chen, K. Cheng, B. Xu, Z. M. Guo, X. M. Liang, M. L. Ye and H. F. Zou, *Anal. Chem.*, 2012, **84**, 5146-5153.

5 J. Zhu, Z. Sun, K. Cheng, R. Chen, M. L. Ye, B. Xu, D.G. Sun, L.M. Wang, J. Liu, F.J. Wang and H.F. Zou, *J. Proteome Res.* 2014, **13**, 1713-1721.

6 Z.A. Lin, J.L. Pang, H.H. Yang, Z.W. Cai, L. Zhang and G.N. Chen, *Chem. Commun.*, 2011, **47**, 9675-9677.

7 L.X. Chen, S.F. Xu and J.H. Li, *Chem Soc Rev.*, 2011, **40**, 2922-2942.

8 R. Schirhagl, *Anal. Chem.*, 2014, **86**, 250-261.

9 Z.C. Liu, Z.Y. Hu, Y. Liu, M.J. Meng, L. Ni, X.G. Meng, G.X. Zhong, F.F. Liu and Y.M. Gao, *RSC Adv.*, 2015, **5**, 52369-52381.

10 W.Y. Fan, M.Q. Gao, M. He, B.B. Chen and B. Hu, *Analyst*, 2015, **140**, 4057-4067.

11 J.H. Tian, J.L. Bai, Y. Peng, Z.W. Qie, Y.F. Zhao, B.A. Ning, D. Xiao and Z.X. Gao, *Analyst*, 2015, **140**, 5301-5307.

12 B.B. Prasad and A. Kumar, *J. Mater. Chem. B*, 2015, **3**, 5864-5876.

13 D.L. Rathbone, *Adv. Drug Delivery Rev.* 2005, **57**, 1854-1874.

14 J.X. Liu, K.G. Yang, Q.L. Deng, Q.R. Li, L.H. Zhang, Z. Liang and Y.K. Zhang, *Chem. Commun.*, 2011, **47**, 3969-3971.

15 L. Qin, X. W. He, W. Zhang, W. Y. Li and Y. K. Zhang, *Anal. Chem.*, 2009, **81**, 7206-7216.

16 F.F. Yang, S. Lin and X.C. Dong, *Chem. Commun.*, 2015, **51**, 7673-7676.

17 S. Shinde, A. Bunschoten, J. A. Kruijtzter, R. M. Liskamp and B. Sellergren, *Angew. Chem., Int. Ed.*, 2012, **51**, 8326-8329.

18 R.Z. Ouyang, J.D. Lei and H.X. Ju, *Chem. Commun.*, 2008, **44**, 5761-5763.

19 Z.W. Xia, Z.A. Lin, Y. Xiao, L. Wang, J. N. Zheng, H.H. Yang and G.N. Chen, *Biosens. Bioelectron.*, 2013, **47**, 120-126.

20 M. Zhang, X.H. Zhang, X.W. He, L.X. Chen and Y.K. Zhang, *Nanoscale*, 2012, **4**, 3141-3147.

21 G.Q. Fu, H.Y. He, Z.H. Chai, H.C. Chen, J. Kong, Y. Wang and Y.Z. Jiang, *Anal. Chem.*, 2011, **83**, 1431-1436.

22 W. Zhang, X.W. He, W.Y. Li and Y.K. Zhang, *Chem. Commun.*, 2012, **48**, 1757-1759.

23 Y.L. Yin, L. Yan, Z. H. Zhang and J. Wang, *Talanta*, 2015, **144**, 671-679.

24 H.Y. Wang, Z.J. Bie, C.C. Lü and Z. Liu, *Chem. Sci.*, 2013, **4**, 4298-4303.

25 H.Y. Li, H.Y. Wang, Y.C. Liu and Z. Liu, *Chem. Commun.*, 2012, **48**, 4115-4117.

26 Z.A. Lin, J.N. Zheng, F. Lin, Z.W. Cai and G.N. Chen, *J. Mater. Chem.*, 2011, **21**, 518-524.

27 L. Li, Y. Lu, Z. Bie, H. Y. Chen and Z. Liu, *Angew. Chem., Int. Ed.*, 2013, **52**, 7451-7454.

28 S.S. Wang, J. Ye, Z.J. Bie and Z. Liu, *Chem. Sci.*, 2014, **5**, 1135-1140.

29 X.D. Bi and Z. Liu, *Anal. Chem.*, 2014, **86**, 959-966.

30 X.D. Bi and Z. Liu, *Anal. Chem.*, 2014, **86**, 12382-12389.

31 Z.J. Bie, Y. Chen, J. Ye, S.S. Wang and Z. Liu, *Angew. Chem., Int. Ed.*, 2015, **54**, 10211-10215.

32 J. Ye, Y. Chen, and Z. Liu, *Angew. Chem., Int. Ed.*, 2014, **53**, 10386-10389.

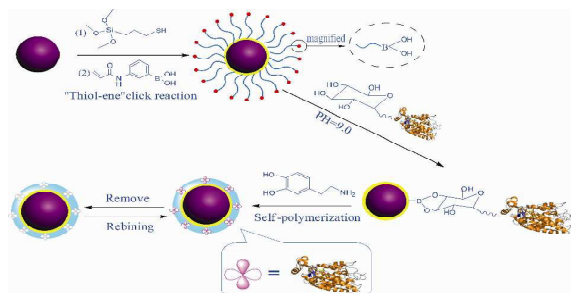
33 Z.A. Lin, L.X. Sun, W. Liu, Z.W. Xia, H.H. Yang and G.N. Chen, *J. Mater. Chem. B* 2014, **2**, 637-643.

34 W. Zhang, W. Liu, P. Li, H.B. Xiao, H. Wang and B. Tang, *Angew. Chem., Int. Ed.*, 2014, **53**, 12489-12493.

Journal Name

- 1 35 C.E. Hoyle and C.N. Bowman, *Angew. Chem., Int. Ed.*, 2010, **49**,
2 1540–1573.
3 36 S.T. Zhang, X.W. He, L.X. Chen and Y.K. Zhang, *New J. Chem.*,
4 2014, **38**, 4212–4218.
5 37 X.H. Zhang, X.W. He, L.X. Chen and Y.K. Zhang, *J. Mater. Chem. B*,
6 2014, **2**, 3254–3262.
7 38 Y.L. Liu, K.L. Ai and L.H. Lu, *Chem. Rev.*, 2014, **114**, 5057–5115.
8 39 R.Z. Ouyang, J.P. Lei and H.X. Ju, *Nanotechnology*, 2010, **21**,
9 185502–185511.
10 40 F. Sahin, E. Turan, H. Tumturk and G. Demirel, *Analyst*, 2012, **137**,
11 5654–5658.
12 41 Y.X. Li, M. Hong, M.M. Miao, Q. Bin, Z.Y. Lin, Z.W. Cai and G.N.
13 Chen, *J. Mater. Chem.*, 2013, **1**, 1044–1051.
14 42 Z.A. Lin, Z.W. Xia, J.N. Zheng, D. Zheng, L. Zhang, H.H. Yang and
15 G.N. Chen, *J. Mater. Chem.*, 2012, **22**, 17914–17922.
16
17
18
19
20
21
22
23
24
25
26
27
28
29
30
31
32
33
34
35
36
37
38
39
40
41
42
43
44
45
46
47
48
49
50
51
52
53
54
55
56
57
58
59
60

Table of contents entry



A novel boronic acid-functionalized molecularly imprinted silica nanoparticles with polydopamine coating was prepared and applied to recognition and enrichment of glycoproteins.